Pergamon

Int. J. Heat Mass Transfer. Vol. 41, No. 1, pp. 33–44, 1998

Printed in Great Britain
0017–9310/98 $19.00+0.00

PII: S0017–9310(97)00117–8

A two-dimensional model of the three-dimensional mixed convection flow of Newtonian and non-Newtonian fluids in a rectangular duct

L. ELLIOTT, D. B. INGHAM† and J. D. WOOD
Department of Applied Mathematical Studies, University of Leeds, Leeds LS2 9JT, U.K.

(*Received* 22 *April* 1997)

Abstract—In this study we investigate the three-dimensional (3-D) mixed convection fluid flow within a horizontal duct, the walls of which are assumed to be maintained at specified constant temperatures. The fluid flowing through the duct is assumed to be steady and laminar and the results presented are mainly concentrated on those obtained when using parameter values that are typically found in hydraulic fractures, a technique used in the oil industry to enhance the production rate of an oil well. The full 3-D governing equations are non-dimensionalized and simplified using a narrow gap type approximation and the resulting two-dimensional (2-D) governing equations are found to be parabolic in the streamwise direction. A stream function is introduced into the solution procedure, which consists of marching streamwise along the duct using a finite-difference technique. Results are found for Newtonian and power-law fluids, as well as Newtonian fluids with a temperature dependent viscosity. © 1997 Elsevier Science Ltd.

1. INTRODUCTION

In this study the problem of obtaining the fluid velocity and the temperature field as the fluid travels along the main body of a rectangular duct, where it is assumed to be two-dimensional (2-D), reduces to solving a parabolic equation in one-dimensional (1-D) space together with a second-order, non-linear partial differential equation. The forced convection problem is the well known Graetz–Nusselt problem for parallel plates [1, 2], and this problem can be solved by the use of the method of separation of variables, as shown by Unwin [3], which reduces the problem to one of a Sturm–Liouville type. In this study, however, a numerical procedure using finite-difference methods was chosen for obtaining the solution, since a numerical method is required in order to incorporate non-Newtonian fluids due to the non-linear coupling of the equations. Examples of existing work associated with the Graetz–Nusselt problem include Prins *et al.* [4], where the leading order terms in the solution were rigorously determined. The influence of streamwise diffusion in the energy was included by Pahor and Strnad [5] and an analytical approach, which yields entrance region solutions with streamwise conduction in the energy for the uniform heat flux boundary condition, was devised by Hsu [6]. The effects of the buoyancy force on the Graetz–Nusselt problem were modelled by Ou *et al.* [7] using a large Prandtl number approximation and they identified the regions where free convection is significant and the behaviour of the local Nusselt number was investigated. This work is particularly relevant to the present study as the Prandtl number is large for the results presented in this paper. More recent work on the Graetz–Nusselt problem includes studies by Aparecido and Cotta [8] on laminar forced convection inside a rectangular duct. In addition, Kim and Özişik [9] investigated conjugate laminar flow convection inside parallel plate and pipe geometries. Their model was subject to a periodically varying inlet temperature with a parabolic fluid velocity profile.

For the streamwise uniform wall temperature condition, the buoyancy effect decreases asymptotically once the fluid goes beyond a critical streamwise location, and this is because the fluid warms up to the wall temperature with increasing streamwise position. The forced convection becomes the dominant mechanism far downstream [10], and the length scale over which the buoyancy force acts is dependent upon the Prandtl number and the Reynolds number. The effects of natural convection in vertical problems has been investigated [11–15].

Numerical simulations of mixed convection boundary-layer flows in ducts were until recently confined to situations which excluded regions of recirculation. Studies undertaken by Aung and Worku [16], describe how asymmetric wall temperatures lead to a skewness in the velocity profile and how, if the magnitude of the buoyancy parameter is sufficiently large, flow reversal can occur at the cold wall. Works by Ingham *et al.* [17] and Heggs *et al.* [18] describe a method of dealing

† Author to whom correspondence should be addressed.

NOMENCLATURE

a^*	height of the model of the fracture
A	matrix of known coefficients
b^*	width of the model of the fracture
$\mathbf{b}$	vector of known coefficients
c^*	length of the model of the fracture
g^*	acceleration due to gravity
Gr'	Grashof number for a generalized Newtonian fluid, $\rho_m^{*2} g^* \beta^* (T_w^* - T_e^*) b^{*2n-1} U^{*2(1-n)} / K'^{*2}$
h	distance between grid nodes in the x-direction
k	distance between grid nodes in the y-direction
K'^*	consistency index for a generalized Newtonian fluid
n	power-law index of fluid
N'	number of grid nodes in the y-direction
p^*	dimensional pressure
p	non-dimensional pressure, $\rho_m^* U^{*2} p/\varepsilon - \rho_m^* z^* g^*$
$\tilde{p}'$	a modified pressure, $Re'p$
Pr'	Prandtl number for a generalized Newtonian fluid, $U^{*n-1} K'^* / \alpha^* \rho_m^* b^{*n-1}$
Re'	Reynolds number for a generalized Newtonian fluid, $\rho_m^* b^{*n-1} U^{*2-n} / K'^*$
T^*	local fluid temperature
T_e^*	temperature of the fluid at the entrance to the duct
T_w^*	average temperature of the duct walls
T_{wa}^*	temperature of the duct walls
u^*, v^*, w^*	the x-, y- and z-components of the fluid velocity
u, v, w	non-dimensional x-, y- and z-components of the fluid velocity, u^*/U^*, $v^*/\varepsilon U^*$, $w^*/\eta U^*$
u_{in}^*	fluid velocity profile at the entrance to the duct
U^*	average streamwise fluid velocity
W	vertical component of the fluid velocity, wRe'/Gr'
x^*	coordinate measuring the horizontal distance streamwise along the duct
x	coordinate measuring the horizontal non-dimensional distance streamwise along the duct, x^*/c^*
y^*	coordinate measuring the horizontal distance across the duct
y	coordinate measuring the horizontal non-dimensional distance across the duct, y^*/b^*
z^*	coordinate measuring the vertical dimensional distance up the duct
z	coordinate measuring the vertical non-dimensional distance up the duct, z^*/a^*.

Greek symbols

α^*	thermal diffusivity of fluid
β^*	coefficient of fluid thermal exapnsion
$\dot{\gamma}^*$	second invariant of the rate of strain tensor
$\dot{\boldsymbol{\gamma}}^*$	rate of strain tensor
$\delta(\theta)$	the non-dimensional temperature dependent viscosity of a Newtonian fluid
ε	ratio of width, b^*, to length, c^*, of the duct
η	ratio of height, a^*, to length, c^*, of the duct
θ	non-dimensional local fluid temperature, $(T^* - T_w^*)/(T_e^* - T_w^*)$
μ^*	fluid viscosity of a generalized Newtonian fluid
ρ^*	fluid density
ρ_m^*	reference density
$\boldsymbol{\tau}^*$	stress tensor
$\boldsymbol{\psi}$	vector of unknown variables.

with flow reversals numerically for different geometries in undeveloped flows and, more recently, reversal of fully developed mixed convection flows in vertical channels were studied by Cheng *et al.* [19].

Few experimental studies exist in the field of mixed convection flows due to the problems that exist with implementing the temperature boundary conditions. However, Wirtz and McKinley [20] investigated the buoyancy effects in a laminar downflow of air between two vertical parallel plates and more recently, Huang *et al.* [21] performed experimental studies of mixed convection flows and heat transfer in a vertical convergent channel.

Relatively little work has been performed on mixed convection, non-Newtonian fluid flows. Bird *et al.* [22] looked at isothermal flows and provided a review for the known exact solutions for the flow of a Bingham plastic in simple geometries, such as the parallel plate duct and the concentric annulus. Wilkinson [23] and Metzner [24] provide summaries of work in forced convection flows on non-Newtonian fluids prior to 1964, whilst McKillop [25], Mahaligan *et al.* [26] and Joshi and Bergles [27] have since extended the work further. Unwin [3] obtain solutions for a power-law fluid for the mixed convection model of a semi-infinite fracture using finite-difference and iterative techniques and Patel and Ingham [28] studied the three-dimensional (3-D) problem of combined convection in a

vertical eccentric annulus for Newtonian fluids, Bingham plastics, power-law fluids and the Herschel–Bulkley model.

In the present study, we undertake the problem of estimating the temperature and fluid flow profiles that exist in a horizontal rectangular duct, the walls of which are assumed to be maintained at specified constant temperatures. As an example, the particular situation of fluid flow in a vertical hydraulic fracture is used to illustrate the results. Hydraulic fracturing, introduced into the oil industry in 1947 [29] is an important technique for enhancing petroleum reserves and increasing the production rate of an oil well. Oil and/or gas pockets in the earth are not always of a concentrated nature and the areas where the oil and/or gas are to be found are called pay zones. In the case of the oil and/or gas being not particularly concentrated in the pay zone it is not efficient to try and collect the oil and/or gas through a well bore alone. To increase the production rate, and thus make the well more cost effective, a greater surface over which to collect the oil and/or gas is created. This greater surface area is obtained by the fracturing process. In this process a fracturing fluid is pumped into a reservoir from a wellbore at the appropriate rates and pressures to both wedge and extend the fracture hydraulically. The fluid is mixed with a propping agent (particles), called a 'proppant'. This fluid carries the proppant deep into the fracture. At the end of the process the fluid is removed from the fracture, by leakoff into the formation and/or flowback into the wellbore, and a propped fracture remains. This propped fracture represents a highly conductive path for oil and/or gas to flow easily from the extremities of the formation into the well. Since we intend to illustrate the results by using the specific case of fluid flow through a hydraulic fracture the values of the parameters appearing in the governing equations and the boundary conditions are chosen to be typical oil-field parameter values. The length of the fracture, c^*, is assumed to be $O(10^2)$m, whereas the fracture width, b^*, is assumed to be much smaller than the fracture length and is typically $O(10^{-2})$m. The height of a typical fracture, a^*, is $O(10)$m. The typical values of the other parameters used in hydraulic fracturing processes are given in Table 1.

Table 1. Typical values of the parameters used in hydraulic fracturing processes

Fluid density, ρ^*	$O(10^3)$ kg m^{-3}
Average streamwise fluid velocity, U^*	$O(10^{-1})$ m s^{-1}
Coefficient of fluid thermal expansion, β^*	$O(10^{-4})$ °C^{-1}
Thermal diffusivity of fluid, α^*	$O(10^{-7})$ m^2 s^{-1}
Newtonian fluid viscosity, μ^*	$O(10^{-1})$ Pa s
Temperature of fracture walls, T^*_{wa}	100–165°C
Temperature of fluid at fracture entrance, T^*_c	40–65°C

The typical values for the Reynolds, Grashof and Prandtl numbers for fluids flowing in fractures and these values are given as follows:

$$O(1) < Re' < O(10)$$

$$O(10^{-1}) < Gr' < O(1)$$

$$O(10^2) < Pr' < O(10^3). \tag{1}$$

The 3-D, horizontal duct is modelled using a cartesian coordinate system (x^*, y^*, z^*), see Fig. 1, with x^* measuring the horizontal distance along the duct, y^* the horizontal distance across the duct and z^* the vertical distance up the duct and where the origin is at the bottom right-hand corner of the entrance to the duct. The temperature of the walls of the duct, T^*_{wa}, is assumed to be a specified constant value, namely, the

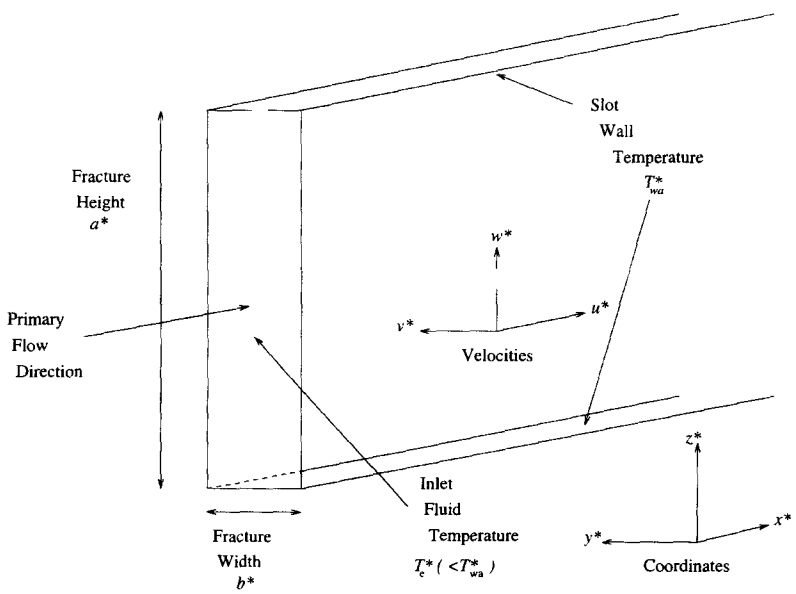

Fig. 1. A model of a fracture.

average temperature of the duct walls, T_w^*, and at the entrance of the duct the temperature of the fluid T_e^* is assumed to be less than T_w^*. The height of the duct, a^*, the width, b^*, and the length, c^*, are taken to be constant.

Fluids with various rheologies are studied, including Newtonian and power-law fluids, as well as Newtonian fluids with a temperature dependent viscosity. The general approach to the solution of this 3-D problem is to make the assumption that the width and height of the duct are much smaller than the length of the duct, thus enabling, after non-dimensionalization, a lubrication type approximation to be made and the quantities appearing in the equations to be asymptotically expanded. The order of the terms in each of the governing equations are investigated and the magnitudes of the non-dimensional numbers created by the non-dimensionalization studied in order to simplify the full 3-D equations to a more manageable, two-dimensional (2-D) form.

2. FORMULATION OF THE TWO-DIMENSIONAL MODEL

Initially the full 3-D governing equations, namely the continuity, momentum and energy equations, are analyzed. The governing equations are non-dimensionalized using the duct length, width and height to scale the x^*, y^* and z^* coordinates, respectively, i.e.

$$x^* = c^* x \quad y^* = b^* y \quad z^* = a^* z \tag{2}$$

where the superscript * denotes a dimensional quantity. The continuity equation is nondimensionalized using the average streamwise fluid velocity, U^*, as a fluid velocity scale in the streamwise direction and the cross-stream components of the fluid velocity are scaled so as to satisfy the continuity equation, namely:

$$u^* = U^* u \quad v^* = \varepsilon U^* v \quad w^* = \eta U^* w \tag{3}$$

where

$$\varepsilon = \frac{b^*}{c^*} \quad \eta = \frac{a^*}{c^*}. \tag{4}$$

The other relevant scalings are given by

$$T^* = T_w^* + (T_e^* - T_w^*)\theta \quad \mu^* = K'^* \left(\frac{b^*}{U^*}\right)^{1-n} \delta(\theta)\dot{\gamma}^{n-1}$$

$$\tau^* = K'^* \left(\frac{U^*}{b^*}\right)^n \tau \quad \dot{\gamma}^* = \dot{\gamma}\frac{U^*}{b^*}$$

$$p^* = \frac{\rho_m^* U^{*2}}{\varepsilon} p - \rho_m^* z^* g^* \tag{5}$$

where T^* is the local fluid temperature, θ is the non-dimensional local fluid temperature, μ^* is the fluid viscosity, K'^* is the consistency index of the fluid, n is the power-law index, $\delta(\theta)$ is the Newtonian viscosity dependence on temperature, $\dot{\gamma}$ is the second invariant of the rate of strain tensor, τ^* is the stress tensor, $\dot{\gamma}^*$ is the rate of strain tensor, p^* is the pressure, ρ_m is the reference density and g^* is the acceleration due to gravity. It should be noted that the viscosity has been scaled so as to describe the viscosity of Newtonian or power-law fluids, or Newtonian fluids with a temperature dependent viscosity. In the limit of $n = 1$ and $\delta(\theta) = 1$, the viscosity, μ^* in expression (5) is that of a Newtonian fluid and K'^* becomes the Newtonian viscosity. Alternatively, in the limit $\delta(\theta) = 1$ the viscosity is that of a power-law fluid, whereas in the limit $n = 1$ the viscosity is that of a Newtonian fluid whose viscosity varies with temperature. With these scalings we can obtain the non-dimensional, governing equations for the flow of fluids through rectangular ducts, namely

$$\frac{\partial u}{\partial x} + \frac{\partial v}{\partial y} + \frac{\partial w}{\partial z} = 0 \tag{6}$$

$$\varepsilon Re' \left\{u\frac{\partial u}{\partial x} + v\frac{\partial u}{\partial y} + w\frac{\partial u}{\partial z}\right\} = -\frac{\partial \tilde{p}}{\partial x} + \varepsilon\frac{\partial \tau_{xx}}{\partial x} + \frac{\partial \tau_{xy}}{\partial y} + \frac{\varepsilon}{\eta}\frac{\partial \tau_{xz}}{\partial z} \tag{7}$$

$$\varepsilon Re' \left\{u\frac{\partial v}{\partial x} + v\frac{\partial v}{\partial y} + w\frac{\partial v}{\partial z}\right\} = -\frac{1}{\varepsilon^2}\frac{\partial \tilde{p}}{\partial y} + \frac{\partial \tau_{yx}}{\partial x} + \frac{1}{\varepsilon}\frac{\partial \tau_{yy}}{\partial y} + \frac{1}{\eta}\frac{\partial \tau_{yz}}{\partial z} \tag{8}$$

$$\varepsilon Re' \left\{u\frac{\partial w}{\partial x} + v\frac{\partial w}{\partial y} + w\frac{\partial w}{\partial z}\right\} = -\frac{1}{\eta^2}\frac{\partial \tilde{p}}{\partial z} + \frac{\varepsilon}{\eta}\frac{\partial \tau_{zx}}{\partial x} + \frac{1}{\eta}\frac{\partial \tau_{yz}}{\partial y} + \frac{\varepsilon}{\eta^2}\frac{\partial \tau_{zz}}{\partial z} - \frac{Gr'}{\eta Re'}\theta \tag{9}$$

$$\varepsilon Re' Pr' \left\{u\frac{\partial \theta}{\partial x} + v\frac{\partial \theta}{\partial y} + w\frac{\partial \theta}{\partial z}\right\} = \varepsilon^2\frac{\partial^2 \theta}{\partial x^2} + \frac{\partial^2 \theta}{\partial y^2} + \frac{\varepsilon^2}{\eta^2}\frac{\partial^2 \theta}{\partial z^2} \tag{10}$$

where $\tilde{p} = Re' p$ is the modified pressure and Gr', Pr' and Re' are the Grashof, Prandtl and Reynolds numbers defined by

$$Gr' = \frac{\rho_m^{*2} g^* \beta^* (T_w^* - T_e^*) b^{*2n+1} U^{*2(1-n)}}{K'^{*2}} \tag{11}$$

$$Pr' = \frac{U^{*n-1} K'^*}{\alpha^* \rho_m^* b^{*n-1}} \tag{12}$$

$$Re' = \frac{\rho_m^* b^{*n} U^{*2-n}}{K'^*} \tag{13}$$

respectively, where β^* is the coefficient of thermal expansion of the fluid and α^* is the thermal diffusivity. Equations (6)–(10) are to be solved along with the integral continuity condition, which ensures continuity of fluid and is given in non-dimensional form by

$$\int_{z=0}^{z=1}\int_{y=0}^{y=1} u\,\mathrm{d}y\,\mathrm{d}z = 1. \tag{14}$$

The non-dimensional forms of the constitutive equation and the rate of strain tensor are given by

$$\boldsymbol{\tau} = \gamma^{n-1}\delta(\theta)\dot{\boldsymbol{\gamma}} \tag{15}$$

$$\dot{\boldsymbol{\gamma}} = \begin{bmatrix} 2\varepsilon\dfrac{\partial u}{\partial x} & \dfrac{\partial u}{\partial y}+\varepsilon^2\dfrac{\partial v}{\partial x} & \dfrac{\varepsilon}{\eta}\dfrac{\partial u}{\partial z}+\varepsilon\eta\dfrac{\partial w}{\partial x} \\ \dfrac{\partial u}{\partial y}+\varepsilon^2\dfrac{\partial v}{\partial x} & 2\varepsilon\dfrac{\partial v}{\partial y} & \dfrac{\varepsilon^2}{\eta}\dfrac{\partial v}{\partial z}+\eta\dfrac{\partial w}{\partial y} \\ \dfrac{\varepsilon}{\eta}\dfrac{\partial u}{\partial z}+\varepsilon\eta\dfrac{\partial w}{\partial x} & \dfrac{\varepsilon^2}{\eta}\dfrac{\partial v}{\partial z}+\eta\dfrac{\partial w}{\partial y} & 2\varepsilon\dfrac{\partial w}{\partial z} \end{bmatrix} \tag{16}$$

respectively.

Equations (6)–(10), along with the integral continuity condition (14), are now to be solved along with the boundary conditions, namely, the no-slip condition on each of the four bounding walls, symmetry about the plane $y = 1/2$, $0 < z < 1$, $x > 0$ and the temperature of the four bounding walls is assumed to be constant and equal to the average temperature of the walls, T_w^*. Thus, the non-dimensional initial and boundary conditions can be summarized as follows:

$$\begin{aligned}
&x = 0 : u = u_{in} \quad v = w = 0 \quad \theta = 1 \\
y = 0 \quad 0 < z < 1 \quad &x > 0 : u = v = w = 0 \quad \theta = 0 \\
y = 1 \quad 0 < z < 1 \quad &x > 0 : u = v = w = 0 \quad \theta = 0 \\
z = 0 \quad 0 < y < 1 \quad &x > 0 : u = v = w = 0 \quad \theta = 0 \\
z = 1 \quad 0 < y < 1 \quad &x > 0 : u = v = w = 0 \quad \theta = 0 \\
y = \frac{1}{2} \quad 0 < z < 1 \quad &x > 0 : \frac{\partial u}{\partial y} = v = \frac{\partial w}{\partial y} = \frac{\partial \theta}{\partial y} = 0.
\end{aligned} \tag{17}$$

By assuming that the quantities ε and η are small and that $0 < \varepsilon \ll \eta \ll 1$, we can proceed to expand the variables, u, v, w, $\tilde{p}$, θ, $\dot{\gamma}$ and τ in powers of ε and η. By doing this we have effectively performed a double expansion of the variables appearing in the governing equations in the following manner:

$$\begin{aligned}
F = {} & F_{00} + \eta F_{01} + \eta^2 F_{02} + \ldots, \\
& + \varepsilon F_{10} + \varepsilon\eta F_{11} + \varepsilon\eta^2 F_{12} + \ldots, \\
& + \varepsilon^2 F_{20} + \varepsilon^2\eta F_{21} + \varepsilon^2\eta^2 F_{22} + \ldots,
\end{aligned} \tag{18}$$

where $F = u$, v, w, $\tilde{p}$, θ, $\dot{\gamma}$ and τ. By substituting expression (18) into the non-dimensional governing equations (6)–(10) we may proceed to set coefficients of powers of ε to zero in order to obtain the leading order equations and if we now look for solutions having a 2-D profile in regions not in the vicinity of the top and bottom duct walls and assume that the quantities u, v, w and θ are independent of z, we obtain the following 2-D governing equations

$$\frac{\partial u_{0q}}{\partial x} + \frac{\partial v_{0q}}{\partial y} = 0 \tag{19}$$

$$0 = -\frac{\partial \tilde{p}_{0q}}{\partial x} + \frac{\partial}{\partial y}\left(\dot{\gamma}_{0q}^{n-1}\,\delta(\theta_{0q})\frac{\partial u_{0q}}{\partial y}\right) \tag{20}$$

$$\begin{aligned}
0 = {} & -\frac{\partial \tilde{p}_{20}}{\partial y} - \eta\frac{\partial \tilde{p}_{21}}{\partial y} - \eta^2\frac{\partial \tilde{p}_{22}}{\partial y} \\
& + \frac{\partial}{\partial x}\left(\dot{\gamma}_{0q}^{n-1}\,\delta(\theta_{0q})\frac{\partial u_{0q}}{\partial y}\right) + 2\frac{\partial}{\partial y}\left(\dot{\gamma}_{0q}^{n-1}\,\delta(\theta_{0q})\frac{\partial v_{0q}}{\partial y}\right)
\end{aligned} \tag{21}$$

$$\begin{aligned}
0 = {} & -\frac{1}{\eta^2}\frac{\partial \tilde{p}_{00}}{\partial z} - \frac{1}{\eta}\frac{\partial \tilde{p}_{01}}{\partial z} - \frac{\partial \tilde{p}_{02}}{\partial z} \\
& + \frac{\partial}{\partial y}\left(\dot{\gamma}_{0q}^{n-1}\,\delta(\theta_{0q})\frac{\partial w_{0q}}{\partial y}\right) - \frac{Gr'}{\eta Re'}\theta_{0q}
\end{aligned} \tag{22}$$

$$\varepsilon Re' Pr'\left\{u_{0q}\frac{\partial \theta_{0q}}{\partial x} + v_{0q}\frac{\partial \theta_{0q}}{\partial y}\right\} = \frac{\partial^2 \theta_{0q}}{\partial y^2} \tag{23}$$

where $F_{0q} = F_{00} + \eta F_{01} + \eta^2 F_{02} + O(\eta^3)$ for $F = u$, v, w, $\tilde{p}$ and θ and terms with coefficients of $\varepsilon Re'$ have been neglected since, for our example of fluid flow in a hydraulic fracture, we are only looking for an order of magnitude estimate and $\varepsilon Re' \leqslant O(10^{-3})$ for parameter values within the typical oilfield range. It should be noted that we have not assumed that $\tilde{p}$ is independent of z so that the effects of the top and bottom bounding walls can be taken into account.

3. THE SOLUTION PROCEDURE

Firstly, for $F = u$, v, w, $\tilde{p}$ and θ we look for the leading order solution in η which satisfies the boundary conditions, so we set $F_{0q} = F_{00}$ in equations (19)–(23). Then by examining the cross-stream components of the momentum equation with respect to the pressure terms we find for $\varepsilon \ll \eta \ll 1$ that

$$\frac{\partial \tilde{p}_{21}}{\partial y} = \frac{\partial \tilde{p}_{22}}{\partial y} = \frac{\partial \tilde{p}_{00}}{\partial z} = \frac{\partial \tilde{p}_{01}}{\partial z} = 0 \tag{24}$$

approximately and hence $\tilde{p}_{00} = \tilde{p}_{00}(x)$. Thus, we can write $\tilde{p}_{00}$ in the form

$$\tilde{p}_{00} = f(x) \tag{25}$$

where $f(x)$ is an unknown function of x. Upon substitution of equation (25) into equation (20) and integrating once with respect to y we obtain

$$-\partial_x(f(x))y + \delta(\theta_{00})\dot{\gamma}_{00}^{n-1}\,\partial_y u_{00} + h(x) = 0 \tag{26}$$

where $h(x)$ is an unknown function of x, since we have already assumed that u_{00} is independent of z. We can now use the symmetry condition in expression (17) at $y = 1/2$ to find $\partial_x(f(x))$ in terms of $h(x)$, namely

$$-\partial_x(f(x))+2h(x)=0 \tag{27}$$

and hence, equation (26) reduces to

$$h(x)(1-2y)+\delta(\theta_{00})\dot{\gamma}_0^{n-1}\,\partial_y u_{00}=0. \tag{28}$$

The governing equations can be put in a more manageable form by expressing $\dot{\gamma}_{00}$ as a function of the temperature and by using Picard iteration on the vertical pressure gradient term, thereby decoupling the vertical component of the momentum equation from the x-component of the momentum equation. This can be achieved by integrating equation (22) once with respect to y to obtain

$$\delta(\theta_{00})\dot{\gamma}_{00}^{n-1}\,\partial_y w_{00}=-\int_y^{1/2}\left(\frac{Gr'}{Re'}\theta_{00}+\frac{\partial\tilde{p}_{02}}{\partial z}\right)\mathrm{d}y' \tag{29}$$

and after squaring and adding equations (28) and (29) we obtain

$$\dot{\gamma}=\left\{\frac{1}{\delta(\theta_0)^2}\left[(h(x)(1-2y))^2+\left(\int_y^{1/2}\left(\frac{Gr'}{Re'}\theta_0+\frac{\partial\tilde{p}_{02}}{\partial z}\right)\mathrm{d}y'\right)^2\right]\right\}^{1/2n}. \tag{30}$$

However, equations (19)–(21) and (23) remain coupled and have to be solved simultaneously.

By introducing the stream function given by

$$u_{00}=\frac{\partial\psi}{\partial y}\quad\text{and}\quad v_{00}=-\frac{\partial\psi}{\partial x} \tag{31}$$

the continuity equation (19) is automatically satisfied and equations (20) and (23) reduce to

$$h(x)(1-2y)+\delta(\theta_{00})\dot{\gamma}_{00}^{n-1}\frac{\partial^2\psi}{\partial y^2}=0 \tag{32}$$

$$\varepsilon Re'Pr'\left\{\frac{\partial\psi}{\partial y}\frac{\partial\theta_{00}}{\partial x}-\frac{\partial\psi}{\partial x}\frac{\partial\theta_{00}}{\partial y}\right\}=\frac{\partial^2\theta_{00}}{\partial y^2}. \tag{33}$$

Equations (32) and (33) represent a coupled set of non-linear, partial differential equations. Since the streamwise coordinate appears only as a first-order derivative, the equations are parabolic in nature and can be solved numerically using a marching procedure. Thus the resulting equations are solved iteratively at each x-location before proceeding streamwise along the duct. Using a regular grid and central differences throughout, along with the Crank–Nicolson method [30], equations (32) and (33) can be written in finite-difference form as follows:

$$h(x_i)(1-2kj)+\delta(\theta_{00i,j})\dot{\gamma}_{00i,j}^{n-1}\left(\frac{\psi_{i,j+1}-2\psi_{i,j}+\psi_{i,j-1}}{k^2}\right)=0 \tag{34}$$

$$\left(\frac{\theta_{00i,j}-\theta_{00i-1,j}}{h}\right)\left\{\frac{1}{2}\left(\frac{\psi_{i,j+1}-\psi_{i,j-1}}{2k}+\frac{\psi_{i-1,j+1}-\psi_{i-1,j-1}}{2k}\right)\right\}-\left(\frac{\psi_{i,j}-\psi_{i-1,j}}{h}\right)\times\left\{\frac{1}{2}\left(\frac{\theta_{00i,j+1}-\theta_{00i,j-1}}{2k}+\frac{\theta_{00i-1,j+1}-\theta_{00i-1,j-1}}{2k}\right)\right\}=\frac{1}{2\varepsilon Re'Pr'}\left(\frac{\theta_{00i,j+1}-2\theta_{00i,j}+\theta_{00i,j-1}}{k^2}+\frac{\theta_{00i-1,j+1}-2\theta_{00i-1,j}+\theta_{00i-1,j-1}}{2k}\right) \tag{35}$$

where h and k are the distances between grid points in the x- and y-direction, respectively. At any given x-location, $h(x)$ is constant and can be found from the stream function boundary conditions at the duct walls, namely

$$\psi=\partial_y\psi=0\quad\text{at}\quad y=0\quad 0<x<\infty \tag{36}$$

$$\psi=1\quad\partial_y\psi=0\quad\text{at}\quad y=1\quad 0<x<\infty. \tag{37}$$

By evaluating equation (34) at the wall $y=0$, we find that $h(x)$ is given by

$$h(x_i)=-2\delta(\theta_{00i,0})\dot{\gamma}_{00i,0}^{n-1}\frac{\psi_{i,1}}{k^2}. \tag{38}$$

Upon substitution of expression (38) into equation (34) we obtain

$$A\boldsymbol{\psi}=\mathbf{b} \tag{39}$$

where A and $\mathbf{b}$ are given by

$$\mathbf{A}=\begin{bmatrix}
-2+\dfrac{\delta(\theta_{00i,0})}{\delta(\theta_{00i,1})}(-2+4k) & 1 & 0 & \cdot & \cdot & \cdot \\
1+\dfrac{\delta(\theta_{00i,0})}{\delta(\theta_{00i,2})}(-2+8k) & -2 & 1 & 0 & \cdot & \cdot \\
\dfrac{\delta(\theta_{00i,0})}{\delta(\theta_{00i,3})}(-2+12k) & 1 & -2 & 1 & \cdot & \cdot \\
\cdot & \cdot & \cdot & \text{etc.} & \cdot & \cdot \\
\dfrac{\delta(\theta_{00i,0})}{\delta(\theta_{00i,N'-1})}(-2+4(n-1)k) & \cdot & \cdot & 0 & 1 & -2
\end{bmatrix}\qquad \mathbf{b}=\begin{bmatrix}0\\0\\\cdot\\\cdot\\-1\end{bmatrix}. \tag{40}$$

The matrix **A** is not diagonally dominant and thus rendering iterative methods on equation (39) susceptible to convergence difficulties. Although equation (39) can be solved by inverting the matrix **A** directly, this results in an excessive amount of computer time and, therefore, a banded solver has been used. Thus, equations (34) and (35) have been solved by marching streamwise along the duct, solving equation (35) at each new x-location to obtain a first approximation for the temperature, then using this approximation to find an estimate for the viscosity and hence the stream function from equation (34). This solution is iterated upon until the sum of the absolute difference between the solutions obtained from two consecutive iterations is less than a very small quantity, say 10^{-7}. Once this is achieved it is assumed that converged solutions have been obtained. Then the solution at the next x-location is sought using the values calculated at the previous x-location. By continuing in this fashion the stream function and the temperature can be found at all locations in the developing region.

If we now proceed to the vertical component of the momentum equation we find we have a vertical pressure gradient that may vary with x without affecting the two-dimensionality of the streamwise component of the fluid velocity, since $\tilde{p}_{02}$ is of a smaller order than $\tilde{p}_{00}$. Although w_{00} is independent of z, to be consistent with the boundary conditions on $z = 0$ and 1 we can enforce that the local vertical volume flux of fluid at any x-location is zero, namely

$$\int_{y=0}^{1} w_{00}\,\mathrm{d}y = 0 \tag{41}$$

and we may now obtain the solution for the vertical component of the fluid velocity. We can split w_{00} into two components, namely

$$w_{00} = w'_{00} + w''_{00} \tag{42}$$

and we may write the vertical component of the momentum equation (22) as

$$0 = \left\{ -\frac{\partial \tilde{p}_{02}}{\partial z} + \frac{\partial}{\partial y}\left(\dot{\gamma}_{00}^{n-1}\,\delta(\theta_{00}) \frac{\partial w'_{00}}{\partial y} \right) \right\} + \left\{ \frac{\partial}{\partial y}\left(\dot{\gamma}_{00}^{n-1}\,\delta(\theta_{00}) \frac{\partial w''_{00}}{\partial y} \right) - \frac{Gr'}{\eta Re'}\theta_{00} \right\}. \tag{43}$$

We can used central finite differences techniques to solve the equation

$$0 = \frac{\partial}{\partial y}\left(\dot{\gamma}_{00}^{n-1}\,\delta(\theta_{00}) \frac{\partial w''_{00}}{\partial y} \right) - \frac{Gr'}{\eta Re'}\theta_{00} \tag{44}$$

and by substituting w''_{00} for w_{00} in expression (41), we obtain

$$\int_{y=0}^{1} w''_{00}\,\mathrm{d}y = B \tag{45}$$

where B is a constant for each x-location which can be found using Simpson's rule. Now since we have obtained v_{00} and u_{00}, we find from equation (21) that $\partial \tilde{p}_{ij}/\partial y = 0$ for all values of i and j. Hence, by adopting Simpson's rule and applying the boundary conditions (17) to the remainder of equation (43), namely

$$0 = -\frac{\partial \tilde{p}_{02}}{\partial z} + \frac{\partial}{\partial y}\left(\dot{\gamma}_{00}^{n-1}\,\delta(\theta_{00}) \frac{\partial w'_{00}}{\partial y} \right) \tag{46}$$

we obtain w'_{00} in terms of $\partial \tilde{p}_{02}/\partial z$. In order to satisfy the integral condition (41), we may now write

$$\int_{y=0}^{1} w'_{00}\,\mathrm{d}y = -B \tag{47}$$

and by applying Simpson's rule once more find $\partial \tilde{p}_{02}/\partial z$. The vertical component of the fluid velocity is now determined from expression (42).

However, if we return to equation (22) for ducts where the duct height is approaching the duct length, i.e. for η approaching unity, we find that it is not true that $\partial \tilde{p}_{00}/\partial z$ (or $\partial \tilde{p}_{01}/\partial z$) $= 0$. In this case $\tilde{p}_{00}$ becomes dependent upon the z-coordinate and we have the situation that the amount of fluid being pushed downwards by the buoyancy force within the fluid is sufficiently great to create pressure gradients, due to the wall at $z = 0$, which are large enough in the vertical direction to affect the streamwise pressure gradient. In this case, the streamwise pressure gradient in the x-component of the momentum equation (20), namely $\partial \tilde{p}_{00}/\partial x$, will depend upon the z-coordinate, thereby rendering 2-D leading order solutions for the streamwise component of the fluid velocity of the form $u_{00}(x, y)$ unobtainable from equation (20).

If we look at typical parameter values for hydraulic fractures, see Section 1.1, we find that $\eta \approx O(10^{-1})$ and since the leading order term in question, namely $\partial \tilde{p}_{02}/\partial z$, has a $1/\eta^2$ as its coefficient, we may conclude that the two-dimensional solutions obtained in this work will be a reasonable approximation (i.e. correct to within about 1%) to the fluid flow found in hydraulic fractures in the regions not in the vicinity of the top and bottom bounding walls.

4. RESULTS AND DISCUSSION

In this section the results for a typical set of oilfield parameter values for various fluids are presented for the fluid flow in a rectangular duct. The initial fluid velocity profile, u_{in}, was chosen to be the fully developed fluid velocity profile, which will, of course, depend upon the value of n. Except very close to the entrance to the duct this will be a good approximation due to the typically high Prandtl number for the case of fluid flows in a hydraulic fracture which results in the fluid boundary-layer developing faster than the thermal boundary-layer at the entrance to the duct. The number of iterations needed at each x-location to obtain accurate solutions to the governing equations

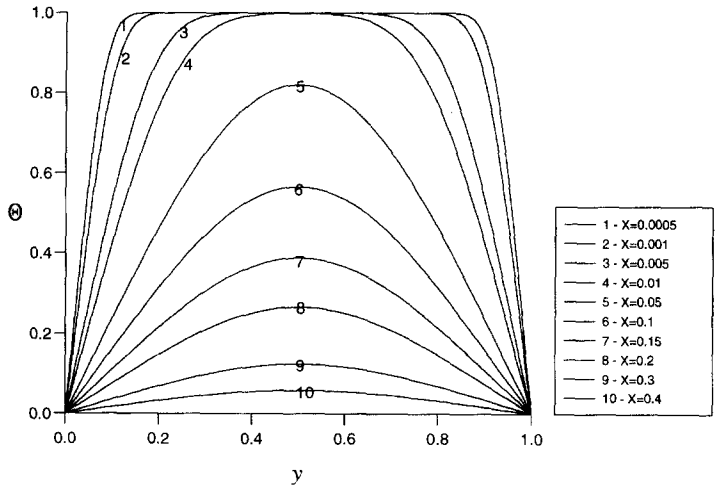

Fig. 2. Temperature distribution across the duct for various values of the distance along the duct, $X = x/(\varepsilon Re' Pr')$, for a Newtonian fluid.

made it desirable to vary the x-step length, h, in order to reduce the computing time. The first 10 x-steps were solved with $h = 10^{-6}$, the following 100 steps with $h = 10^{-5}$ and the remainder of the results were calculated with $h = 10^{-4}$. All the results were calculated with $N' = 200$, where N' is the number of grid points in the cross-stream plane, and comparisons with finer and coarser grids indicated that the solutions obtained were within the desired convergence requirements.

Since the parameters are chosen to take values in or near the range found in hydraulic fracture treatments, we take the buoyancy parameter, $Gr'/\eta Re'$, to be in the range $0.1 \leqslant Gr'/\eta Re' \leqslant 10$, the parameter $\varepsilon Re' Pr'$ to be in the range $0.1 \leqslant \varepsilon Re' Pr' \leqslant 10$ and $\varepsilon = 10^{-4}$. The ratio of the duct height to the duct width, η/ε, is assumed to be $O(10^{-1})$.

4.1. *Newtonian and power-law fluids*

For a Newtonian fluid with a constant viscosity it is found that the streamwise pressure gradient is a constant and, therefore, the u and v components can be found analytically and are given by

$$u = 6y(1-y) \quad v = 0 \tag{48}$$

respectively.

Figure 2 shows the non-dimensional temperature distribution for a Newtonian fluid for various values of the distance along the duct, $x/(\varepsilon Re' Pr')$. It should be noted that for a Newtonian fluid the duct width appears as a squared quantity in the parameter $\varepsilon Re' Pr'$, whereas the quantities U^*, c^* and α^* appear as linear factors, and hence a small change in b^* can have a large effect on the temperature distribution and the length of the developing region. Since $\varepsilon Re' Pr'$ is the only parameter that appears in the energy equation (33), and only as a coefficient of the inertia term on the left-hand side of equation, we can re-scale the x-coordinate by taking $X = x/(\varepsilon Re' Pr')$ and so the parameter $\varepsilon Re' Pr'$ is scaled out of the equation. It is observed that the initial uniform temperature profile, namely $\theta(0, y) = 1$ asymptotically approaches $\theta(\infty, y) = 0$ as the distance along the duct increases. Further, it is found that the length of the developing region for a fluid to be within about 1% of the temperature of the duct walls is $x/(\varepsilon Re' Pr') = 0.676$.

The parameter Gr'/Re' depends linearly on the quantities U^*, T_c^*, T_w^*, β^*, ρ_m^* and K^* and quadratically on b^*. Hence, small variations in the duct width may result in large differences in the buoyancy force within the fluid. As was the situation for the parameter $\varepsilon Re' Pr'$ in the energy equation, we can scale the parameter Gr'/Re' out of the vertical component of the momentum equation by re-scaling the quantities w_{00} and $\partial \tilde{p}_{02}/\partial z$ with Gr'/Re'. The vertical component of the fluid velocity profiles is shown in Fig. 3 for various values of the distance along the duct, $x/(\varepsilon Re' Pr')$. It is observed that the fluid moves upwards near the hot walls and downwards in the central region of the duct. Further, as the fluid moves streamwise this effect increases in magnitude until a critical x-location is reached, whence the vertical component of the fluid velocity asymptotically decreases in magnitude to zero. We note that the vertical component of the fluid velocity is approximately three orders of magnitude smaller than the streamwise component of the fluid velocity.

Figures 4 and 5 show comparisons between the solutions obtained for the vertical component of the fluid velocity for a Newtonian fluid on the plane $z = 1/2$, $0 < y < 1$ at the locations $x = 0.01$ and $x = 0.11$, respectively, on using the 3-D model as described by Wood *et al.* [31] for duct height to width aspect ratios of 1, 2, 4, 8 and 64 and the solutions obtained at the corresponding locations using the 2-D model as described in this paper, where the parameters $\varepsilon Re'$, $\varepsilon Re' Pr'$ and $Gr'/(\eta Re')$ are 0.001, 0.5 and 1, respectively. In each figure we find that the solutions obtained with the 3-D model approach those obtained with the 2-D model as the duct height to width aspect

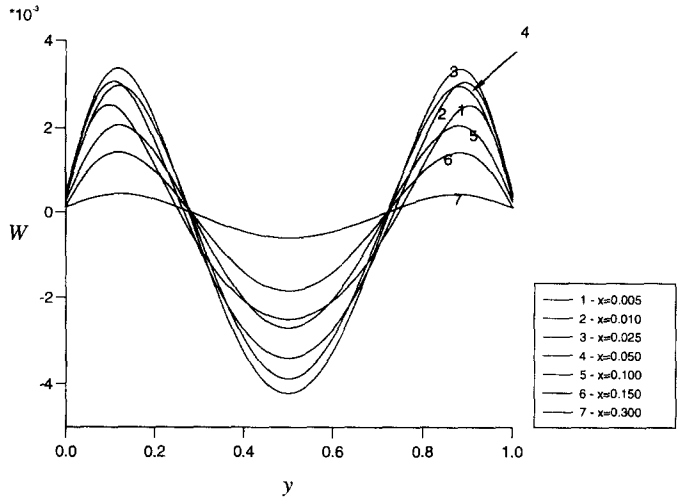

Fig. 3. Vertical component of the fluid velocity profiles, $W = wRe'/Gr'$, across the duct for various values of the distance along the duct, $X = x/(\varepsilon Re'Pr')$, for a Newtonian fluid.

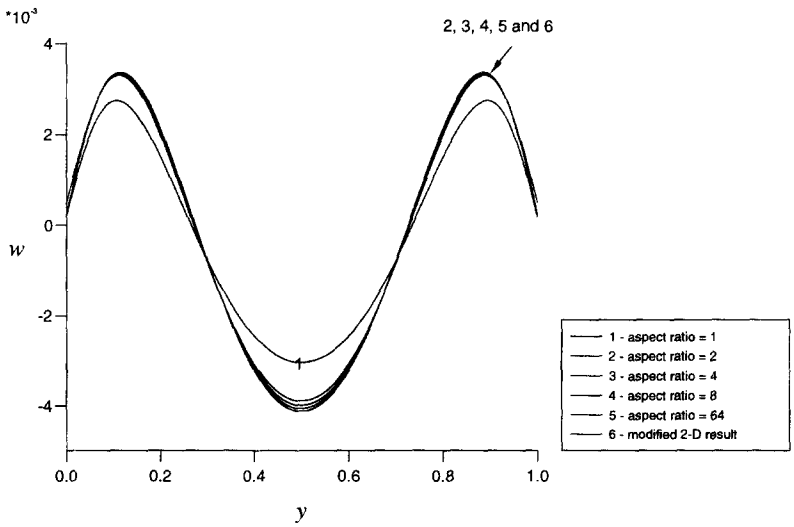

Fig. 4. The variation of the vertical component of the fluid velocity for a Newtonian fluid as calculated using the two- and three-dimensional models for various values of the duct height to width aspect ratio on the line given by $z = 1/2$, $0 < y < 1$, $x = 0.01$, where the parameters $\varepsilon Re'$, $\varepsilon Re'Pr'$ and $Gr'/(\eta Re')$ are 0.001, 0.5 and 1, respectively.

ratio increases. In Fig. 4, we find that the solutions in each case are almost identical, except for the case of the square duct geometry. However, in Fig. 5 we find that the solutions obtained for the vertical component of the fluid velocity with the three-dimensional model increase in magnitude as the aspect ratio increases to about four, after which the solutions asymptotically decrease in magnitude with increasing duct height to width aspect ratio towards the solutions obtained with the 2-D model. This is due to the influence of the heat transfer from the bounding walls at $z = 0$ and 1 on the local temperature field reaching a critical level, with respect to the local temperature gradients within the fluid, at a value of the duct height to width aspect ratio of about four.

It we now look at the fluid velocity field for power-law fluids, we find that the streamwise and horizontal cross-stream components of the fluid velocity are virtually identical at each x-location along the duct, as in the Newtonian case, and approximately equal to the fully developed initial u and v-velocity profiles specified at the entrance of the developing region. Figure 6 shows the variation of the vertical component of the fluid velocity across the duct at different x-locations for a power-law fluid with a power-law index equal to 0.5, where $Gr'/Re' = 1$ and $\varepsilon Re'Pr' = 1.0$. We can see that, as for Newtonian fluids, the fluid moves upwards near the walls at $y = 0$ and 1 and downwards in the central region of the duct. As the local fluid temperature asymptotically tends towards the temperature of the duct walls with increasing values of x, the magnitude of the vertical component of the fluid velocity asymptotically decreases towards zero. For power-law fluids with $n < 1$, we find the increase in

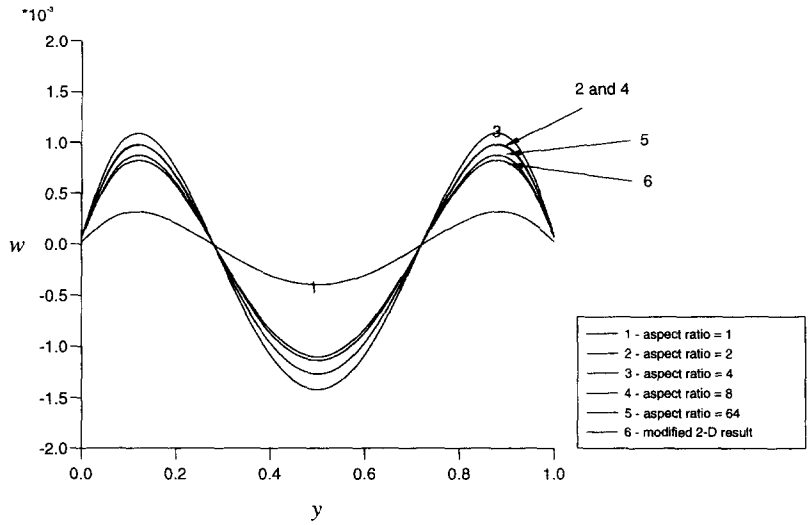

Fig. 5. The variation of the vertical component of the fluid velocity for a Newtonian fluid as calculated using the two- and three-dimensional models for various values of the duct height to width aspect ratio on the line given by $z = 1/2$, $0 < y < 1$, $x = 0.11$, where the parameters $\varepsilon Re'$, $\varepsilon Re' Pr'$ and $Gr'/(\eta Re')$ are 0.001, 0.5 and 1, respectively.

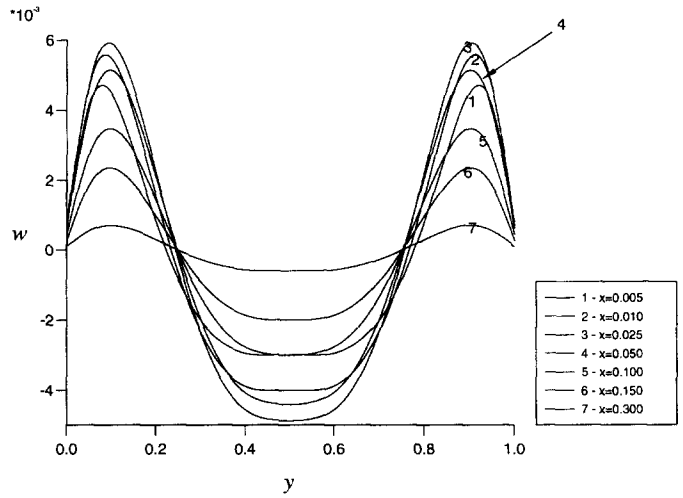

Fig. 6. Vertical component of the fluid velocity profiles across the duct at various x-locations along the duct for a power-law fluid with $n = 0.5$.

non-Newtonian behaviour as n decreases results in more 'peaked' and 'flatter' profiles near the duct walls and in the central region of the duct, respectively. We note also that the magnitude of the maximum vertical component of the fluid velocity in Fig. 6 is larger than in the corresponding Newtonian case. This is because the viscosity decreases with decreasing values of n in the regions near the walls at $y = 0$ and 1 due to the large shear rates. We find that the opposite is true for power-law fluids with $n > 1$, with the profiles of the vertical component of the fluid velocity becoming more 'peaked' in the central region of the duct and 'flatter' near the walls at $y = 0$ and 1 and the magnitude of the vertical component of the fluid velocity at a particular x-location becoming smaller than those found in the corresponding Newtonian case. Again, we find good agreement with the results obtained with the 3-D model of Wood *et al.* [31]. Figure 7 shows a comparison between the solutions obtained for the vertical component of the fluid velocity for a power-law fluid with $n = 0.5$ on the plane $z = 1/2$, $0 < y < 1$ at the x-location $x = 0.01$ using the 3-D model, as described by Wood *et al.* [31], for duct height to width aspect ratios of 1, 2, 4, 8 and 64 and the solutions obtained at the corresponding location by the 2-D model of this paper, where the parameters $\varepsilon Re'$, $\varepsilon Re' Pr'$ and $Gr'/(\eta Re')$ take the values 0.001, 0.5 and 1, respectively.

For power-law fluids we can re-scale x with the parameter $\varepsilon Re' Pr'$ in the energy equation (23) and re-scale w_{00} with the parameter $Gr'/(\eta Re')$ in the z-component of the momentum equation (22) and

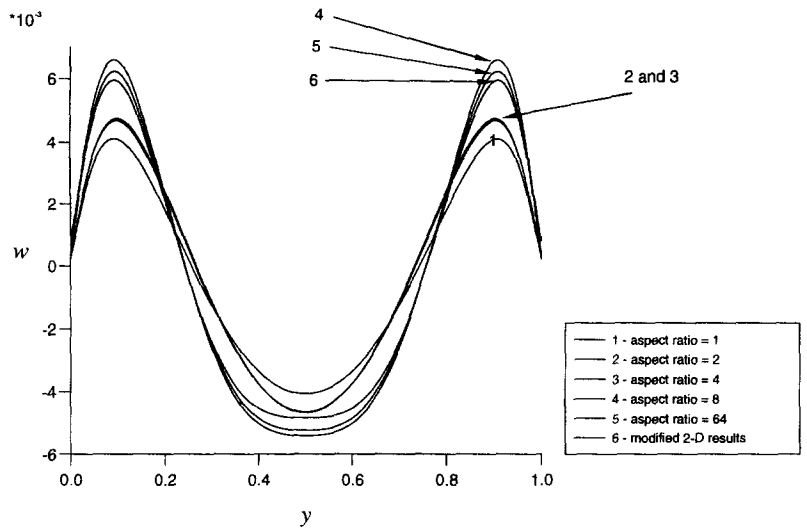

Fig. 7. The variation of the vertical component of the fluid velocity for a power-law fluid as calculated using the two- and three-dimensional models for various values of the duct height to width aspect ratio on the line given by $z = 1/2$, $0 < y < 1$, $x = 0.01$, where the parameters n, $\varepsilon Re'$, $\varepsilon Re'Pr'$ and $Gr'/(\eta Re')$ are 0.5, 0.001, 0.5 and 1, respectively.

obtain solutions for the temperature distribution and the vertical component of the fluid velocity. For a power-law fluids with a fixed value of n we find that with these scalings, the temperature distribution and the vertical component of the fluid velocity are almost identical for all values of the parameters $\varepsilon Re'Pr'$ and $Gr'/(\eta Re')$ within the range of values investigated in this paper.

4.2. *Newtonian fluids with a temperature dependent viscosity*

For a Newtonian fluid with a temperature dependent viscosity, as discussed by Wood *et al.* [31], the buoyancy driven motion is not the only cross-stream motion since fluid is being drawn towards the top and bottom bounding walls of the duct in order to satisfy the continuity of fluid. Thus, when the fluid has a large temperature dependent viscosity, this cross-stream motion cannot be estimated using this 2-D model.

5. CONCLUSIONS

The full, steady, 3-D, laminar, mixed convection flow of fluids in a horizontal duct of constant width and constant wall temperatures has been examined. By performing a double asymptotic expansion in terms of the two aspect ratios of the duct, namely the parameters ε and η, and setting all the terms involving $\partial/\partial z$ and $\partial^2/\partial z^2$ to be identically zero, we are able to obtain a 2-D model such that for $\eta \ll 1$ the vertical pressure gradient may depend upon x without destroying the two-dimensionality of the governing equations. For Newtonian and power-law fluids, the results obtained with this 2-D model are found to be in good agreement with the full 3-D solutions which were obtained previously in regions of the duct not in the vicinity of the top and bottom duct walls as the duct height to width aspect ratio increases. However, it should be noted that for Newtonian fluids with a large temperature dependent viscosity, this 2-D model cannot predict the fluid flow since a buoyancy driven flow is not the only cross-stream motion for these fluids.

For ducts where the height is sufficiently less than the length, the 2-D results obtained in this paper are a good approximation for the fluid flow in 3-D ducts in regions of the duct not in the vicinity of the top and bottom duct walls. However, as the duct height approaches the magnitude of the duct length, the 2-D model investigated breaks down due to the vertical pressure gradient approaching the order of the streamwise pressure gradient. In this case, the simplifying double expansion procedure breaks down and 2-D solutions for the fluid velocity and temperature fields cannot be calculated.

Acknowledgements—Part of this research was funded by the EPSRC and Schlumberger Cambridge Research.

REFERENCES

1. Shah, R. K. and London, A. L., *Advances in Heat Transfer, Laminar Flow Forced Convection in Ducts*. Academic Press, London, 1978.
2. Kakaç, S., Shah, R. K. and Aung, W., Handbook of single-phase convective heat transfer. *Mixed Convection in Internal Flow*, Chapter 15. Wiley, New York, 1987.
3. Unwin, A. T., The mixed convection flow of Newtonian and non-Newtonian fluids in a vertical fracture. Internal Report, SCR Ltd, Cambridge.
4. Prins, J. A., Mulder, J. and Schenk, J., Heat transfer in laminar flow between parallel plates. *Applied Science Research*, 1951, **A2**, 431–438.
5. Pahor, S. and Strnad, J., A note on heat transfer in laminar flow through a gap. *Applied Science Research*, 1961, **10**, 81–84.

6. Hsu, C.-J., An exact mathematical solution for entrance-region laminar heat transfer with axial conduction. *Applied Science Research*, 1967, **17**, 359–376.
7. Ou, J.-W., Cheng, K. C. and Lin, R.-C., Natural convection effets on Graetz problem in horizontal rectangular channels with uniform wall temperature for large Pr. *International Journal of Heat and Mass Transfer*, 1974, **17**, 835–843.
8. Aparecido, J. B. and Cotta, R. M., Thermally developing laminar flow inside rectangular ducts. *International Journal of Heat and Mass Transfer*, 1990, **33**, 341–347.
9. Kim, W. S. and Özişik, M. N., Conjugate laminar forced convection in ducts with periodic variation of inlet temperature. *International Journal of Heat Fluid and Flow*, 1990, **11**, 311–320.
10. Hieber, C. A. and Sreenwasan, S. K., Mixed convection in an isothermally heated horizontal pipe. *International Journal of Heat and Mass Transfer*, 1974, **17**, 1337–1348.
11. DeYoung, S. H. and Scheele, G. F., Natural convection distorted non-Newtonian flow in a vertical pipe. *AIChE Journal*, 1970, **16**, 712–717.
12. Marner, W. J. and McMillan, H. K., Combined free and forced laminar non-Newtonian convection in a vertical tube with constant wall temperature. *Chemical Engineering Science*, 1972, **27**, 473–488.
13. Gori, F., Effects of variable physical properties in laminar flow of a pseudoplastic fluid. *International Journal of Heat and Mass Transfer*, 1978, **21**, 247–250.
14. Lin, T. F., Yin, C. P. and Yan, W. M., Transient laminar mixed convection heat transfer in a vertical plat duct. *Journal of Heat Transfer*, 1991, **113**, 384–390.
15. Patel, N. and Ingham, D. B., The combined convection flow of a Bingham plastic in an oil well. *Proceedings of the* 1993 *IChemE Research Event*, Vol. 1, 1993, pp. 284–286.
16. Aung, W. and Worku, G., Developing flow and flow reversal in a vertical channel with asymmetric wall temperatures. *ASME Journal of Heat Transfer*, 1986, **108**, 229–304.
17. Ingham, D. B., Keen, D. J. and Heggs, P. J., Two-dimensional combined convection in vertical parallel plate ducts, including situations of flow reversal. *International Journal of Numerical Methods in Engineering*, 1988, **26**, 1645–1664.
18. Heggs, P. J., Ingham, D. B. and Keen, D.J., The effects of heat conduction in the wall on the development of recirculating combined convection flows in vertical tubes. *International Journal of Heat and Mass Transfer*, 1990, **33**, 517–528.
19. Cheng, C. H., Kou, H. S. and Huang, W. H., Flow reversal and heat transfer of fully developed mixed convection in vertical channels. *Journal of Thermophysical Heat Transfer*, 1990, **3**, 375–383.
20. Wirtz, R. A. and McKinley, P., Buoyancy effects on downwards laminar convection between parallel plates. In *Fundamentals of Forced and Mixed Convection*, eds F. A. Kulacki and R. D. Boyd, Vol. 42. ASME, New York, 1995, pp. 105–112.
21. Huang, T. M., Gau, C. and Aung, W., Mixed convection flow and heat transfer in a heated vertical convergent channel. *International Journal of Heat and Mass Transfer*, 1995, **38**, 2445–2456.
22. Bird, R. B., Dai, G. C. and Yarusso, B. J., The rheology and flow of viscoplastic materials. *Review of Chemical Engineering*, 1983, **1**, 36–69.
23. Wilkinson, R. L., *Non-Newtonian Fluids, Fluid Mechanics, Mixing and Heat Transfer*. Pergamon Press, Oxford, 1960.
24. Metzner, A. B., Heat transfer in non-Newtonian fluids. *Advances in Heat Transfer*, 1965, **2**, 357–394.
25. McKillop, A. A., Heat transfer for laminar flow of non-Newtonian fluids in entrance region of a tube. *International Journal of Heat and Mass Transfer*, 1964, **7**, 853–862.
26. Mahaligan, R., Tilton, L. O. and Coulson, J. M., Heat transfer in laminar flow of non-Newtonian fluids. *Chemical Engineering Science*, 1975, **30**, 921–929.
27. Joshi, S. D. and Bergles, A. E., Analytical study of laminar flow heat transfer of a pseudoplastic fluid in tubes with uniform wall temperature. *AIChE Symposium Series, Heat Transfer, Milwaukee*, 1981, **77**(208), 114–122.
28. Patel, N. and Ingham, D. B., Mixed convection flow of a Bingham plastic in an eccentric annulus. *International Journal of Heat and Fluid Flow*, 1994, **15**, 132–141.
29. Veatch, R. W., Moschovidis, Z. A. and Fast, R., Recent advances in hydraulic fracturing. Monograph Vol. 12, Society of Petroleum Engineers Inc, 1989.
30. Smith, G. D., *Numerical Solution of Partial Differential Equations*. Oxford University Press, New York, 1985.
31. Elliott, L., Ingham, D. B. and Wood, J. D., The mixed convection flow of Newtonian and non-Newtonian fluids in a horizontal rectangular duct. *Journal of Numerical Heat Transfer* (accepted for publication).